Potentiometric and Multinuclear NMR Study of the Binary and Ternary Uranium(VI)−L−Fluoride Systems, Where L Is α-Hydroxycarboxylate or Glycine

Zoltán Szabó* and Ingmar Grenthe*

Department of Chemistry, Inorganic Chemistry, Royal Institute of Technology (KTH), S-100 44 Stockholm, Sweden

Received April 17, 2000

Equilibria, structures, and ligand-exchange dynamics in binary and ternary U(VI)−L−F^- systems, where L is glycolate, α-hydroxyisobutyrate, or glycine, have been investigated in 1.0 M $NaClO_4$ by potentiometry and ^1H, ^{17}O, and ^{19}F NMR spectroscopy. L may be bonded in two ways: either through the carboxylate end or by the formation of a chelate. In the glycolate system, the chelate is formed by proton dissociation from the α-hydroxy group at around pH 3, indicating a dramatic increase, a factor of at least 10^{13}, of its dissociation constant on coordination to uranium(VI). The L exchange in carboxylate-coordinated $UO_2LF_3^{2-}$ follows an Eigen−Wilkins mechanism, as previously found for acetate. The water exchange rate, $k_{aq} = 4.2 \times 10^5\ s^{-1}$, is in excellent agreement with the value determined earlier for UO_2^{2+}(aq). The ligand-exchange dynamics of $UO_2(O-CH_2-COO)_2F^{3-}$ and the activation parameters for the fluoride exchange in D_2O ($k_{obs} = 12\ s^{-1}$, $\Delta H^{\ddagger} = 45.8 \pm 2.2$ kJ mol^{-1}, and $\Delta S^{\ddagger} = -55.8 \pm 3.6$ J K^{-1} mol^{-1}) are very similar to those in the corresponding oxalate complex, with two parallel pathways, one for fluoride and one for the α-oxocarboxylate. The same is true for the L exchange in $UO_2(O-CH_2-COO)_2^{2-}$ and $UO_2(oxalate)_2^{2-}$. The exchange of α-oxocarboxylate takes place by a proton-assisted chelate ring opening followed by dissociation. Because we cannot decide if there is also a parallel H^+-independent pathway, only an upper limit for the rate constant, $k_1 < 1.2\ s^{-1}$, can be given. This value is smaller than those in previously studied ternary systems. Equilibria and dynamics in the ternary uranium(VI)−glycine−fluoride system, investigated by ^{19}F NMR spectroscopy, indicate the formation of one major ternary complex, $UO_2LF_3^{2-}$, and one binary complex, UO_2L_2 (L = $H_2N-CH_2COO^-$), with chelate-bonded glycine; $\log \beta(9) = 13.80 \pm 0.05$ for the equilibrium $UO_2^{2+} + H_2N-CH_2COO^- + 3F^- = UO_2(H_2N-CH_2COO)F_3^{2-}$ and $\log \beta(11) = 13.0 \pm 0.05$ for the reaction $UO_2^{2+} + 2H_2N-CH_2COO^- = UO_2(H_2N-CH_2COO)_2$. The glycinate exchange consists of a ring opening followed by proton-assisted steps. The rate of ring opening, $139 \pm 9\ s^{-1}$, is independent of both the concentration of H^+ and the solvent, H_2O or D_2O.

Introduction

In previous papers, we have discussed the rates and mechanisms of inter- and intramolecular ligand-exchange reactions in dioxouranium(VI) complexes.[1−3] A prerequisite for these studies was the possibility of using different NMR-active nuclei to probe the reactions at differing reactant concentrations and varying pH. To study the behavior of a certain ligand, L, we found it practical to use ternary complexes, which in addition to L also contain coordinated fluoride. Fluoride is an excellent NMR probe; at the same time, it prevents the formation of hydroxide complexes and the precipitation of hydrous oxides at higher pH levels. By using this technique for bidentate ligands, it was possible to study the rate and mechanism of chelate ring opening/closure, to identify isomers, and to suggest mechanisms for their interconversion. In the present study, we continue this line of investigation using glycolate, α-hydroxyisobutyrate, and glycine. We determine if the mode of coordination of the ligand takes place at the carboxylate end only or if a chelate involving a second donor atom is formed. The hydroxy group is a very weak acid[4] with a pK value in the range 17−20. It is well-known that the more acidic aromatic hydroxy groups can be deprotonated when coordinated to metal ions, for example, in complexes of 5-sulfosalicylate;[5,6] deprotonation of aliphatic OH groups in ligands that contain more than one carboxylate group, such as tartrate, malate,[7,8] and citrate,[8−10] are also well documented. Nunes and Gil[11] have given the most conclusive evidence for reactions of this type. Examples of deprotonation of aliphatic α-hydroxy monocarboxylates are scarce, with one example in lanthanide glycolate complexes[12] and a second in the uranium(VI) complexes studied by Kakihana et al.[13] The formation of complexes of this type is expected to have large effects on both the stability constants and the ligand-exchange dynamics in these systems, with implications for their use in separation processes.[14]

* To whom correspondence should be addressed. E-mail: zoltan@inorchem.kth.se, ingmarg@inorg.kth.se. Fax: 46−8−212626.

(1) Szabó, Z.; Aas, W.; Grenthe, I. *Inorg. Chem.* **1997**, *36*, 5369.
(2) Szabó, Z.; Grenthe, I. *Inorg. Chem.* **1998**, *37*, 6214.
(3) Aas, W.; Szabó, Z.; Grenthe, I. *J. Chem. Soc., Dalton Trans.* **1999**, 1311.
(4) Silva, C. O.; Silva, E. C.; Nascimento, M. A. C. *J. Phys. Chem. A* **2000**, *104*, 2402.
(5) Havel, J.; Sommer, L. *Collect. Czech. Chem. Commun.* **1968**, *33*, 529.
(6) Jahagirdar, D. V.; Khanolkar, D. D. *J. Inorg. Nucl. Chem.* **1973**, *35*, 921.
(7) Rajan, K. S.; Martell, A. E. *J. Inorg. Nucl. Chem.* **1964**, *26*, 1927.
(8) Markovits, G.; Klotz, P.; Newman, L. *Inorg. Chem.* **1972**, *11*, 2405.
(9) Rajan, K. S.; Martell, A. E. *Inorg. Chem.* **1965**, *4*, 462.
(10) Ohyoshi, E.; Oda, J.; Ohyoshi, A. *Bull. Chem. Soc. Jpn.* **1975**, *48*, 227.
(11) Nunes, M. T.; Gil, V. M. S. *Inorg. Chim. Acta* **1987**, *129*, 283.
(12) Grenthe, I. *Acta Chem. Scand.* **1969**, *23*, 1253.
(13) Kakihana, M.; Nagumo, T.; Okamoto, M.; Kakihana, H. *J. Phys. Chem.* **1987**, *91*, 6128.

10.1021/ic000400n CCC: $19.00
Published on Web 10/06/2000

The mode of coordination of α-hydroxy acids in actinide complexes has been discussed by Ahrland,[15] who stated, "though still marked the chelate effect is evidently much smaller for MO_2^{2+} than for M^{3+}", whereas Starý and Balek[16] concluded that for U(VI) the increase in stability between acetate and α-hydroxycarboxylates was due to the formation of chelates for the latter. There are few investigations of complexes between UO_2^{2+} and amino acids.[17−19] This is mainly due to the difficulty in avoiding the formation of hydrolysis products caused by the strong basicity of the amino group. This problem can be avoided by using fluoride as a second ligand, as indicated above.

Experimental Section

Solutions. Stock solutions of uranium(VI) perchlorate and perchloric acid were prepared as described elsewhere.[20] The sodium perchlorate was prepared from $NaClO_4 \cdot H_2O$ (analytical grade) and analyzed by weighing samples dried at 120 °C. NaF, glycolic acid, α-hydroxyisobutyric acid, and glycine were of analytical grade. The nitrogen gas was purified by successively passing it through 10% NaOH, 10% H_2SO_4, 1 M $NaClO_4$, and a G4 filter. In the preparation of the NMR samples, $HClO_4$ and NaOH were used to adjust pH. ^{17}O NMR measurements were performed by using ^{17}O-enriched samples (10%). The enrichment of the oxygens of uranium(VI) was accomplished[21] by using $H_2{}^{17}O$.

Potentiometric Titrations. All electromotive force (emf) measurements were performed in a thermostated box at 25.00 ± 0.05 °C and monitored by an automated titration system. The glass, fluoride, and reference (Ag/AgCl) electrodes were from Metrohm. The equilibrium criterion was an emf that remained constant within 0.1 mV/h for both electrodes; this took 20−30 min after each addition of titrant. All experiments were made in a $NaClO_4$ medium at a constant sodium concentration, $[Na^+] = 1.00$ M. The binary uranium(VI)−glycolate or uranium(VI)−α-hydroxyisobutyrate systems were investigated in the following way: A known amount of $HClO_4$ was added to an acidic uranyl solution, which was then titrated with NaOH in order to calibrate the glass electrode. Both the initial proton concentration (H_0) and the standard potential to the glass electrode (E_0) were determined from these data using a Gran plot.[22] An appropriate amount of glycolic or α-hydroxyisobutyric acid was then added to the test solution, and the titration with NaOH was continued until precipitation occurred. The ternary uranyl−fluoride−glycolate system was investigated in the same way; after determination of E_0 and H_0 for the starting solution, glycolic acid was added, followed by titration with NaOH until pH ≈ 5−5.5. These data were used to determine the equilibrium constants of the binary UO_2^{2+}−L system. After a known amount of NaF was added, the titration was continued by adding NaOH and measuring the potential of both the glass and fluoride electrodes. By adding fluoride at pH ≈ 5, one avoids the presence of HF, which corrodes the glass electrode. The fluoride membrane electrode was calibrated before and after the experiments with a standard NaF solution. The titrations were repeated using different starting concentrations of U(VI), glycolate, and fluoride. In the ternary uranyl−fluoride−α-hydroxyisobutyrate system, we used a different method. First, the binary U(VI)−L system was studied as described above until the equivalence point of the ligand acid had been reached. The titration was then continued, this time by adding a NaF solution. The protonation constants for glycolic and α-hydroxyisobutyric acids were determined in separate experiments, and their values agree very well with those in the literature.[23] The equilibrium constants were calculated and refined using PC-LAKE,[24] a least-squares program using the total hydrogen ion concentration (in the glycolate system) or the total fluoride concentration (in the α-hydroxyisobutyrate system) as error-carrying variables.

NMR Measurements. The NMR spectra were recorded on Bruker AM400 and DMX500 spectrometers at −5 °C, in general using 5% D_2O solutions to get locked mode. The temperature was checked using the chemical shift of methanol.[25] The test solutions were measured in 5-mm (for ^1H and ^{19}F) or 5- and 10-mm (for ^{17}O) NMR tubes. The ^1H NMR spectra recorded at 500.1 MHz were referenced to internal tetramethylsilane. The ^{19}F NMR spectra recorded at 470.5 MHz were referenced to an aqueous solution of 0.01 M NaF in 1 M $NaClO_4$ (pH = 12) at 25 °C; the ^{17}O NMR spectra (54.2 or 67.8 MHz) were referenced to water at 25 °C. The proton concentration ($-\log[H^+]$) in the NMR samples was measured using a pH meter (Orion) and a HF-resistant combined glass electrode (Ingold) in which the inner solution of KCl was replaced by 1 M NaCl to avoid precipitation of $KClO_4$ in the liquid junction. The proton concentration was calculated from the measured $-\log[H^+]$ corrected for the "Irving factor"[26] in the working media. The value of $-\log[D^+]$ in pure D_2O solvent was calculated as described before.[21] The line widths were determined by fitting a Lorentzian curve to the experimental signal using the WIN-NMR software.[27] Magnetization transfer experiments were performed using Gaussian pulses. The ligand-exchange reactions were studied using different dynamic NMR methods that are well documented in the literature.[28]

Results and Discussion

(A) Constitution. The stoichiometry and the equilibrium constants of the different complexes were determined by potentiometry. Exceptions are the data for $UO_2(OCH_2COO)F_3^{3-}$ and the complexes in the glycine system, which were based on ^{19}F NMR integrals. The equilibrium constants refer to the following reactions:

$$UO_2^{2+} + pL^- \rightleftharpoons UO_2(H_{-1})_qL_p^{2-p-q} + qH^+ \qquad (1)$$

and

$$nUO_2^{2+} + pL^- + rF^- \rightleftharpoons (UO_2)_n(H_{-1})_qL_pF_r^{2n-p-q-r} + qH^+ \qquad (2)$$

where L^- denotes glycolate or α-hydroxyisobutyrate.

By potentiometry, one cannot distinguish between deprotonation of the OH group in the ligand and from coordinated water. This information is provided by the NMR data. The equilibrium constants and constitution of the different complexes, denoted **1**−**11**, are given in Table 1 and Chart 1.

A measure of the agreement between the chemical model proposed and the experimental data is given by the quantities $C_{H,total}$ and $C_{F,total}$ as a function of $-\log[H^+]$ and $-\log[F^-]$, respectively (cf. Supporting Information, S1 and S2). The deviations are small and essentially random. The good agreement between model and experimental data results in a small estimated uncertainty of the constants, given as 3σ, where σ is the estimated standard deviation in the least-squares refinement. All complexes have also been identified from NMR, and their

(14) Choppin, G. R.; Rydberg, J. *Nuclear Chemistry Theory and Applications*; Pergamon Press: Oxford, 1983.
(15) Ahrland, S. *Acta Chem. Scand.* **1953**, *7*, 485.
(16) Starý, J.; Balek, V. *Collect. Czech. Chem. Commun.* **1962**, *27*, 809.
(17) Cefola, M.; Taylor, R. C.; Gentile, P. S.; Celiano, A. V. *J. Phys. Chem.* **1962**, *66*, 790.
(18) Lagrange, P.; Schneider, M.; Zare, K.; Lagrange, J. *Polyhedron* **1994**, *13*, 861.
(19) Lagrange, P.; Schneider, M.; Lagrange, J. *J. Chim. Phys. Phys.-Chim. Biol.* **1998**, *95*, 2280.
(20) Ciavatta, L.; Ferri, D.; Grenthe, I.; Salvatore, F. *Inorg. Chem.* **1981**, *20*, 463.
(21) Szabó, Z.; Glaser, J.; Grenthe, I. *Inorg. Chem.* **1996**, *35*, 2036.
(22) Gran, G. *Analyst* **1952**, *77*, 661.
(23) Perrin, D. D. *Stability Constants of Metal−Ion Complexes, Part B: Organic Ligands*; Pergamon Press: Oxford, 1983.
(24) Ingri, N.; Andersson, I.; Pettersson, L.; Yagasaki, A.; Andersson, L.; Holmström, K. *Acta Chem. Scand.* **1996**, *50*, 717.
(25) Geet, A. L. V. *Anal. Chem.* **1970**, *42*, 679.
(26) Irving, H. M.; Miles, M. G.; Pettit, L. D. *Anal. Chim. Acta* **1967**, *38*, 475.
(27) WIN-NMR, 6.0 ed.; Bruker-Franzen Analytik GmbH.
(28) Szabó, Z.; Glaser, J. *Magn. Reson. Chem.* **1995**, *33*, 20.

Table 1. Values of log β for the Complexes[a]

complex	glycolate	α-hydroxyisobutyrate
1	2.38[b]	3.32 ± 0.02
2	3.95[b]	5.25 ± 0.02
3	5.16[b]	6.95 ± 0.03
4	−1.26 ± 0.07	< −2
5	0.19 ± 0.09	0.59 ± 0.03
6	−4.17 ± 0.04	−5.23 ± 0.04
7	10.36 ± 0.09	10.96 ± 0.04
8	11.89 ± 0.10	12.96 ± 0.06
9	5.1± 0.10[c]	
10	11.09 ± 0.10	
11	−2.40 ± 0.07	

[a] The protonation constants of the ligands determined in this study are log β_H(glycolate) = 3.59 ± 0.01 and log β_H(α-hydroxyisobutyrate) = 3.785 ± 0.005, where the uncertainty is equal to 3σ. The equilibrium constants for the formation of binary fluoride complexes $UO_2F_n^{2-n}$, n = 1, 2, or 3, taken from Ahrland and Kullberg (ref 37) are log β_1 = 4.54, log β_2 = 7.98, and log β_3 = 10.41. [b] Literature values. [c] Based on NMR data.

Chart 1. [a]

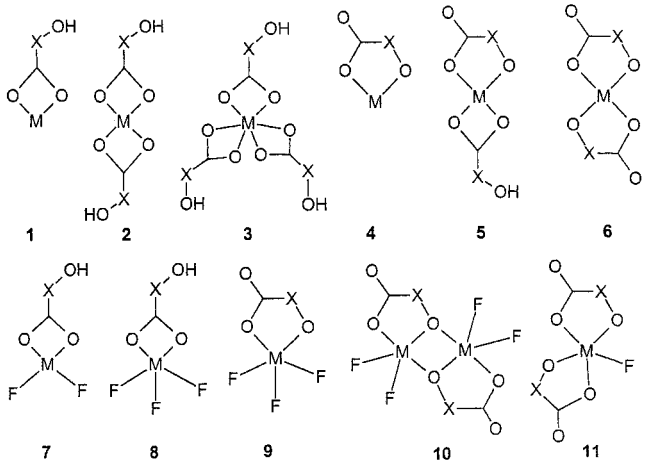

[a] M = UO_2^{2+}, X = $-CH_2-$ (glycolate) or $-C(CH_3)_2-$ (α-hydroxyisobutyrate)

peak integrals give an independent confirmation of the chemical model proposed.

The equilibrium constants indicate a very large increase in the pK value for the dissociation of the α-hydroxy proton, from 17 or higher in free glycolate to 3.64 on coordination to uranium(VI), an increase of at least 13 orders of magnitude. The binary α-hydroxyisobutyrate complexes are more stable than the corresponding glycolate complexes at pH < 5. Our NMR data show that this is not due to differences in the ability to form chelates—both ligands coordinate at the carboxylate end only—but is presumably a result of the inductive effect obtained by replacing the CH_2 protons in glycolate with methyl groups.

The uranium(VI)−glycine system has been described in two previous investigations by Cefola et al.[17] and Lagrange et al.[18,19] The equilibrium constants deduced from the NMR measurements are in better agreement with those obtained by Cefola et al. than with the data reported by Lagrange et al., which are 3 orders of magnitude larger. We believe that the latter constants are in error for the following reasons: Lagrange et al. have used spectrophotometry in their study. The experiments seem impeccable, but the data interpretation neglected the formation of hydroxo complexes, with the argument that they are present in small amounts. This is true, but the molar absorptivity of these complexes is much higher[29] than those of UO_2^{2+} and the glycine complexes. Hence their contribution to the measured absorptivity cannot be neglected. The speciation of the test solutions using the equilibrium constants of Lagrange et al. is not in agreement with the NMR data.

The potentiometric and NMR data, vide infra, indicate very clearly that the glycolate and α-hydroxyisobutyrate ligands are bonded through the carboxylate end in complexes **1**−**3**, **5**, **7**, and **8**. The observed variations in the equilibrium constants between acetate, glycolate, and α-hydroxyisobutyrate are presumably a result of different inductive effects on the carboxylate group, with stronger complexes formed by the electron-donating substituents. The amino group in glycine is a stronger electron donor than the OH group, and we therefore expect that glycinate coordinated only through its carboxylate end forms stronger complexes than any of the α-hydroxycarboxylates; an educated guess is a log K value between 4 and 4.5. The fact that no such complexes can be observed is due to the strong basicity of the amino group, resulting in the formation of a "zwitterion" at moderate pH and a chelate at higher pH. The inductive effect is apparent in both the binary and the ternary complexes, as seen from Table 1.

(B) NMR Measurements. (1) The Uranium(VI)−Glycolate and Uranium(VI)−Glycolate−Fluoride Systems. ^{17}O and ^{1}H NMR spectra were recorded for the binary system and are shown in the Supporting Information (S3 and S4). As a result of fast exchange between the different complexes and the free ligand, one ^{17}O NMR peak was observed for complexes **1**, **2**, and **3**, in which only the carboxylate group is coordinated. At higher pH, separate narrow peaks for the chelate complexes **4**, **5**, and **6** were observed. This indicates that deprotonation and coordination of the OH group result in a dramatic decrease in the rate of ligand exchange. Only one peak is observed for complexes **4** and **5**. This is a result of fast exchange of the carboxylate-bonded ligand. The ^{1}H NMR spectra are in accordance with the ^{17}O observations. Fast exchange between the free ligand and the carboxylate-coordinated species results in only one methylene proton peak. Its line width is increasing with pH, as a result of the formation of **5**. The chemical shift of the carboxylate-coordinated ligand in the latter complex is somewhat different from those in **1**, **2**, and **3** but still close enough to the shift of the free ligand to result in only one exchange-averaged peak. The line width of the free ligand becomes very narrow after pH 7 as a result of the formation of complex **6**, in which the ligand exchange is slow. The chelate-bonded ligand gives two additional peaks at significantly higher chemical shifts; one is common for **4** and **5**, and the other is for **6**.

In the ternary systems, ^{19}F NMR spectroscopy was essential to obtain structure and dynamic information. The pH dependence of the ^{19}F NMR spectra and the uranium distribution diagram can be seen in Figures 1 and 2. At lower pH, beside the peaks of the binary fluoride complexes (UO_2F_2(aq), $UO_2F_3^-$, and $UO_2F_4^{2-}$), broad signals for **7** and **8** can be observed. In these complexes, the dynamics of the ligand exchange is very similar to that in the corresponding acetate system. The broad peak for **7** is a result of a fast site exchange caused by glycolate and/or water exchange. For complex **8**, two peaks can be observed in a ratio of 2:1 like those in the acetate system. It was not possible to obtain quantitative information on the concentration dependence of the rate of exchange, because the smaller peak overlaps the one from $UO_2F_3^-$. At pH > 5, chelate complexes **9**, **10**, and **11** are formed, each with separate narrow peaks. As a result of its different chemical environment, the fluoride in complex **9** gives three separate signals with large chemical shift differ-

(29) Meinrath, G. *Radiochim. Acta* **1997**, *77*, 221.

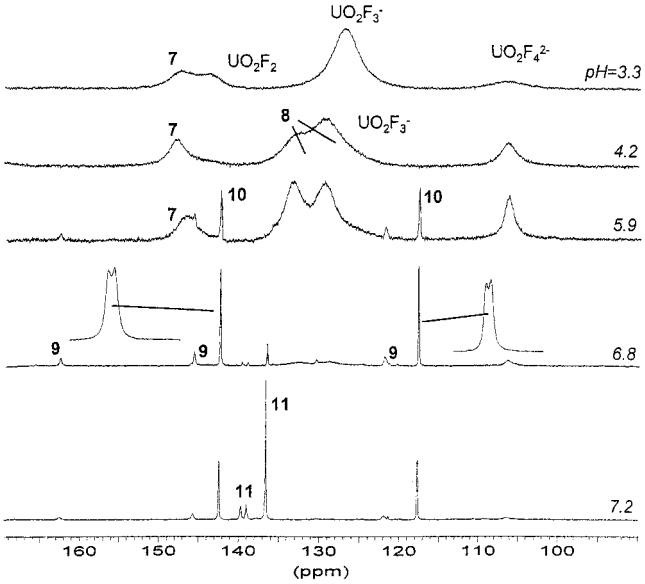

Figure 1. pH dependence of the ^{19}F NMR spectra for the ternary U(VI)−glycolate−fluoride system (10 mM UO_2^{2+}, 100 mM glycolic acid, and 50 mM fluoride, 268 K). The insets show the coupling of 27.6 Hz between the fluoride sites in complex **10**.

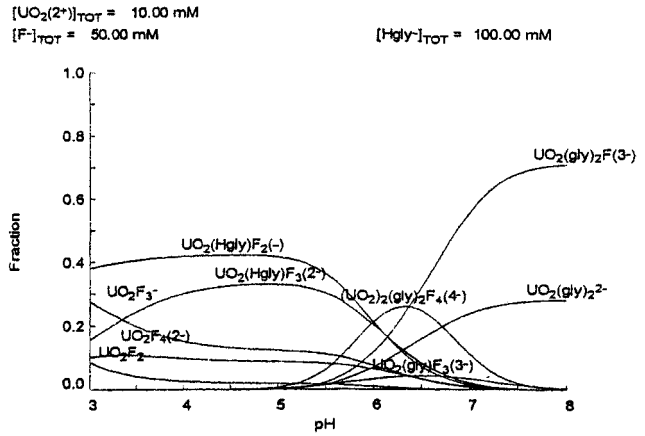

Figure 2. Uranium(VI) equilibrium distribution diagram as a function of pH for the ternary U(VI)−glycolate−fluoride system formed by the total concentrations of 10 mM UO_2^{2+}, 100 mM glycolic acid, and 50 mM fluoride.

ences. Similar observations were made in the corresponding picolinate complexes.[1] Because of the small amount of **9** in the test solutions, it was not possible to determine the rates of ligand exchange. In the dimer **10**, there are two fluoride signals with the same intensity and a coupling constant of 27.6 Hz. The structure of the sodium salt of this complex has been investigated by single-crystal X-ray diffraction.[30] At pH ∼8, the dominant ternary complex is **11**, with three possible isomers. The very different intensities of the three narrow signals indicate significant differences in the thermodynamic stability of the isomers as well as slow exchange between them.

In the ^{17}O NMR spectra, one common peak was observed for the binary fluoride complexes and the carboxylate-coordinated ternary complexes (**7** and **8**). When the pH was increased, separate peaks were observed for complexes **10** and **11**. Because of its low concentration, the ^{17}O signal of **9** was not detected (Supporting Information, S5).

The ^{1}H NMR spectra are in accordance with the previous measurements. One averaged peak can be observed for the free glycolate and the carboxylate-coordinated ternary complexes, whereas separate peaks were observed for the chelate complexes. The line width of the free ligand increases with the concentration of **7** and **8** (Supporting Information, S6).

(a) Equilibrium Dynamics. The glycolate exchange for $UO_2(O-CH_2-COO)_2^{2-}$ and $UO_2(O-CH_2-COO)_2F^{3-}$ was studied using ^{1}H NMR spectra in D_2O. The line width of the proton signal in the binary complex increased with the free glycolate concentration, whereas it remained constant in the ternary system. A plot of k_{obs} versus the equilibrium concentration of glycolate is linear (Supporting Information, S7). The slope gives the rate constant 567 ± 13 M^{-1} s^{-1} for the reaction

$$UO_2(O-CH_2-COO)_2^{2-} + HO^*-CH_2-COO^- \rightleftharpoons UO_2(O^*-CH_2-COO)_2^{2-} + HO-CH_2\text{-}COO^- \quad (3)$$

In $UO_2(O-CH_2-COO)_2F^{3-}$, the line width of the ^{1}H signal was independent of the free glycolate concentration. The rate of exchange between coordinated and free glycolate was therefore determined by magnetization transfer and found to be 1.2 s^{-1}. The rate of fluoride exchange as determined by magnetization transfer in the same test solutions was 12 s^{-1}, very close to the value found for other ternary fluoride complexes. These results indicate that the glycolate and fluoride exchanges follow two parallel pathways as in the corresponding oxalate system.[2,3]

The activation parameters for both the fluoride and the glycolate exchange were determined from the temperature dependence of the ^{19}F and ^{1}H NMR spectra. For the fluoride exchange, we found $\Delta H^{\ddagger} = 45.8 \pm 2.2$ kJ mol^{-1} and $\Delta S^{\ddagger} = -55.8 \pm 3.6$ J K^{-1} mol^{-1}, and for the glycolate exchange, the results were $\Delta H^{\ddagger} = 55.8 \pm 0.8$ kJ mol^{-1} and $\Delta S^{\ddagger} = -42.1 \pm 2.7$ J K^{-1} mol^{-1}, where the uncertainty is the estimated standard deviation in the least-squares fit (Supporting Information, S8).

(2) Ligand Exchange Mechanisms. In addition to reaction 3, we studied the following reactions:

$$UO_2(O-CH_2-COO)_2F^{3-} + HO^*-CH_2-COO^- \rightleftharpoons UO_2(O^*-CH_2-COO)_2F^{3-} + HO-CH_2-COO^- \quad (4)$$

$$UO_2(O-CH_2-COO)_2F^{3-} + {}^*F^- \rightleftharpoons UO_2(O-CH_2-COO)_2{}^*F^- + F^- \quad (5)$$

These reactions are similar to the exchange of oxalate and fluoride in $UO_2(oxalate)_2^{2-}$ and $UO_2(oxalate)_2F^{3-}$, studied previously.[2] A similar mechanistic scheme (Scheme 1) will therefore be used but with the important difference that the glycolate exchange also involves a protonation/deprotonation of the ligand. This was investigated by varying the pH between 6.8 and 8, where the line shape of complex **11** turned out to be constant. The mechanistic implications of this will be discussed below with the ternary glycine system.

Assuming an Eigen−Wilkins mechanism for reaction 3 with an outer sphere equilibrium constant $K_{os} = 0.018$, we find a rate of water exchange $k_{H_2O} = 3.15 \times 10^4$ s^{-1}, 1 order of magnitude smaller than that in other uranium(VI) systems,[31] including the corresponding oxalate system. This indicates a different reaction mechanism in which other steps such as ring opening, internal proton transfer, and so forth may play a role. Both the rate constant and the activation parameters for the

(30) Farkas, I.; Csöregh, I.; Szabó, Z. *Acta Chem. Scand.* **1999**, *53*, 1009.

(31) Farkas, I.; Bányai, I.; Szabó, Z.; Wahlgren, U.; Grenthe, I. *Inorg. Chem.* **2000**, *39*, 799.

Scheme 1

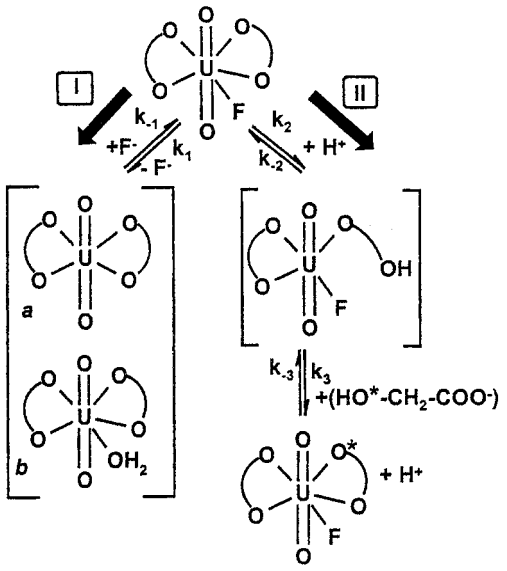

fluoride exchange (eq 5) are within the experimental errors, identical with those in the corresponding oxalate complex; cf. Scheme 1. This is an additional indication that the fluoride exchange in these ternary complexes is not strongly influenced by the second ligand. The activation parameters for the glycolate exchange (eq 4) are significantly different from those in the oxalate system. This is not surprising in view of the protonation/deprotonation of the ligand in the glycolate system.

(3) The Uranium(VI)−α-Hydroxyisobutyrate and Uranium(VI)−α-Hydroxyisobutyrate−Fluoride Systems. As observed in the binary glycolate system, only one exchange-averaged peak was observed in the ^{17}O NMR spectra of the binary uranium(VI)−α-hydroxyisobutyrate system at lower pH (Supporting Information, S9). When the pH is increased, the line width first increases as result of the exchange between the free aqua ion and the first carboxylate-coordinated complex **1**. The peak gets successively narrower as the pH increases, presumably as a result of the disappearance of UO_2^{2+} as the complexes **1**, **2**, and **3** are formed. The chemical shift difference between the aquo ion and the first complex seems to be larger than that between the complexes. At pH > 5.5, separate peaks were observed for complexes **5** and **6** as a result of the slow exchange. ^{1}H NMR spectra are not very informative because of the large concentration difference between the coordinated and the free ligand and the small chemical shift difference between their methyl signals. As a result, individual peaks cannot be resolved for the chelate complexes.

The ternary system was investigated by both ^{19}F and ^{17}O NMR spectroscopy. In one set of experiments, the pH was changed, and in the other the total fluoride concentration was varied at an approximately constant pH of ∼6. The pH-dependent ^{19}F NMR spectra and an equilibrium uranium distribution diagram are shown in the Supporting Information, S10 and S11. In addition to the peaks of the binary fluoride complexes, only the signals of the carboxylate-coordinated complexes **7** and **8** were observed. Complex **7** has one relatively broad peak, whereas **8**, like the glycolate and acetate systems,[3] has two peaks with a 2:1 intensity ratio. These peaks are narrower than those in the corresponding acetate complex, indicating a slower exchange with the free ligand. Three additional peaks with the same (small) intensity, presumably from **9**, were observed at higher pH. The ^{17}O NMR spectra at different pH levels contain only one narrow peak, confirming that the complexes with deprotonated OH groups are present only in small amounts.

(a) Equilibrium Dynamics. The deprotonation of the OH group is insignificant in the ternary system and only the carboxylate-coordinated $UO_2(HO{-}IBA)F_3^{2-}$ (IBA = $-C(CH_3)_2-$COO) complex is present even at higher pH; that is, the system is similar to the corresponding acetate system, with exchange of L and F^- following two separate pathways. In the acetate system, the dissociation of the acetate is much faster than that of fluoride, with $UO_2F_3(H_2O)_2^{2-}$ as a reactant in the reverse reaction; cf. eq 6. The two broad fluorine signals in a ratio of 2:1 for $UO_2(HO{-}IBA)F_3^{2-}$ indicate a dissociation reaction:

$$UO_2(HO{-}IBA)F_3^{2-} \underset{k_{-1}}{\overset{k_1}{\rightleftharpoons}} UO_2F_2(H_2O)_2^{-} + HO{-}IBA^{-} \quad (6)$$

In the reverse reaction, the line width of $UO_2F_3^-$ depends linearly on the free ligand concentration, as found by plotting k_{obs} ($=\pi\,\Delta\nu(UO_2F_3^-)$) versus the equilibrium concentration of α-hydroxyisobutyrate (Supporting Information, S7). From the slope, we obtain $k_{-1} = (3.1 \pm 0.1) \times 10^4$ M^{-1} s^{-1}, almost the same as in the acetate case (2.5×10^4 M^{-1} s^{-1}). Given the Eigen−Wilkins model with $K_{os} = 0.074$, the water exchange rate is equal to $k_{aq} = 4.2 \times 10^5$ s^{-1}, in excellent agreement with the value[31] determined earlier at the same temperature for UO_2^{2+}. This indicates a common mechanism for the reverse reaction in both systems. The rate of the dissociation of α-hydroxyisobutyrate, calculated from the stability constants, is

$$k_1 = k_{-1}[UO_2F_3^-][\,HO{-}IBA^-]/[\,UO_2(HO{-}IBA)F_3^{2-}] = k_{-1}\beta(UO_2F_3^-)/\beta(UO_2(HO{-}IBA)F_3^{2-}) = 250\ s^{-1} \quad (7)$$

This value is in accordance with the one calculated from the observed line broadening for $UO_2(HO{-}IBA)F_3^{2-}$ and is smaller than that in the acetate system (∼1300 s^{-1}).

(4) The Ternary Uranium(VI)−Glycine−Fluoride System. Both equilibria and dynamics were investigated by ^{19}F NMR spectroscopy, the latter in both H_2O and D_2O. The spectra, measured as a function of pH from 2 to 8.5 at different total concentrations of fluoride and glycine, indicate the formation of one major ternary complex, $UO_2LF_3^{2-}$ (Supporting Information, S12). The presence of three ^{19}F peaks of the same magnitude confirms structure **9**, where L is chelate-bonded. All peaks have the same line width, indicating the same dynamics at all sites. The equilibrium constant $\log K_8 = 1.89 \pm 0.05$ for the reaction

$$UO_2F_4^{2-} + H_2N{-}CH_2COO^- \rightleftharpoons UO_2(H_2N{-}CH_2COO)F_3^{2-} + F^- \quad (8)$$

was calculated from the peak integrals of the fluoride species and the concentration of free glycinate (the error indicates the error from integration). Using the known equilibrium constant[3] for the formation of $UO_2F_4^{2-}$, we calculated $\log \beta_9 = 13.80 \pm 0.05$ for the reaction

$$UO_2^{2+} + H_2N{-}CH_2COO^- + 3F^- \rightleftharpoons UO_2(H_2N{-}CH_2COO)F_3^{2-} \quad (9)$$

The only fluoride-containing species at higher pH are one ternary complex, $UO_2LF_3^{2-}$ (L = $H_2N{-}CH_2COO^-$), and $UO_2F_4^{2-}$. In addition, there is no evidence for hydroxide complexes. Hence the total concentration of uranium(VI), $[U]_{tot}$,

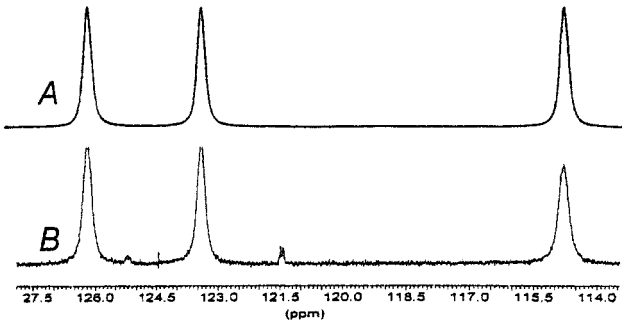

Figure 3. Measured (B) and calculated (A) ^{19}F NMR spectra for the peaks of $UO_2(glycine)F_3^{2-}$ (10 mM UO_2^{2+}, 300 mM glycine, and 200 mM fluoride, pH = 8.5) The calculation of the pseudo-first-order rate constants is detailed in the text. The free fluoride signal at around 0 ppm is not shown.

is equal to $[UO_2LF_3^{2-}] + [UO_2F_4^{2-}] + [UO_2L^-] + [UO_2L_2]$. At the high concentration of free glycinate in the test solutions, $[UO_2L^-] \ll [UO_2L_2]$. Using this experimental information, we can calculate the equilibrium constant for the reaction

$$UO_2LF_3^{2-} + L^- \rightleftharpoons UO_2L_2 + 3F^- \qquad (10)$$

as $\log K_{10} = -0.80 \pm 0.05$. By use of this value and $\log \beta_9 = 13.80 \pm 0.05$, we obtain the equilibrium constant $\log \beta_{11} = 13.0 \pm 0.05$ for the reaction

$$UO_2^{2+} + 2L^- \rightleftharpoons UO_2L_2 \qquad (11)$$

We used the same protonation constants for glycine as in Lagrange et al.[18]

(a) Equilibrium Dynamics. The NMR line shape of coordinated fluoride is affected by all inter- and intramolecular ligand-exchange processes.[1] The interpretation of the kinetic data is facilitated if one can use more than one nuclear probe. Unfortunately, ^1H NMR spectroscopy could not be used in this case because the methylene signal for the coordinated ligand coincides with the water peak in H_2O and D_2O. We therefore had to rely on ^{19}F NMR spectroscopy alone (magnetization transfer and line shape analysis) to obtain information on both the fluoride and glycine exchanges. The magnetization transfer experiments were made using a test solution in which the predominant species are $UO_2(H_2N-CH_2COO)F_3^{2-}$ and free fluoride (Figure 3). The small amount of $UO_2F_4^{2-}$ (<5%) can be neglected in the data treatment. By inverting all fluoride signals from the ternary complex and free fluoride and studying their time dependence, we could separate the inter- and intramolecular exchange reactions and determine their pseudo-first-order rate constants. This was done by a nonlinear fitting procedure[3] (see Figure 4), which gave the rate constants 48 and 70 s^{-1} for the inter- and intramolecular fluoride exchange reactions, respectively, as described in the following. It is not straightforward to calculate the rate of glycine exchange from the ^{19}F line width because the coupling between the fluoride sites has to be considered. The following procedure was used: Model spectra were calculated[32] at different values of the rate constant for glycinate exchange using a coupling constant of 35 Hz (observed earlier in similar complexes[1]) and the experimental rate constant 48 s^{-1} for the exchange between free and bonded fluoride. The glycine exchange rate was then determined by comparing the measured and calculated ^{19}F line shapes and varying the rate constant for the exchange until they were the same (Figure 3).

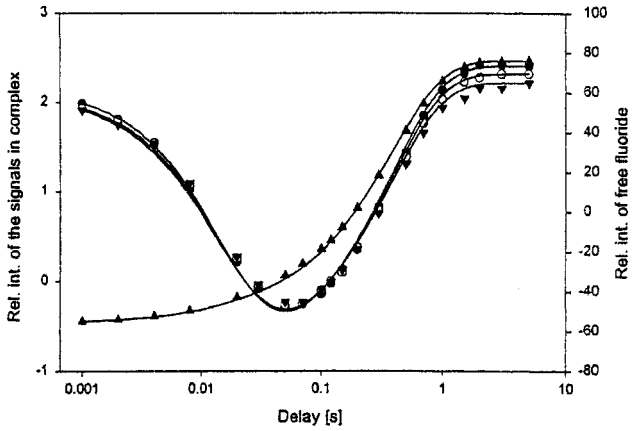

Figure 4. Plots of peak intensity from a ^{19}F NMR magnetization transfer experiment for $UO_2(glycine)F_3^{2-}$ (●, ▼, and ○) against variable delay after selective inversion of the free fluoride signal (▲). The solid lines are generated by a simultaneous analysis of all the experiments inverting the signals of the complex.

The amino group is a strong base, and we therefore investigated the pH dependence of the rate of exchange from ^{19}F spectra at different pH values between 6.5 and 8.5. These boundaries were set by precipitation at high pH and insufficient concentration of the complex below pH 6.5. We observed that the line width of coordinated fluoride increased with decreasing pH, which we interpreted as the result of a fast proton-catalyzed glycine exchange. Similar observations were made in D_2O, where we also noted a pronounced reverse isotope effect.

A "saturation" type of curve (S12) was observed when k_{obs} for the glycine exchange is plotted versus pH or pD. The following empirical rate law describes the observations:

$$k_{obs} = a \times [H^+]/(1 + b \times [H^+]) \qquad (12)$$

The results can now be discussed using Scheme 2, which is analogous to the one used previously[1,2] but with the addition of a proton-assisted pathway.

The coordinated amino group is not available for proton attack; hence the first step is a ring opening/closure with rate constants k_1 and k_{-1}, respectively. The ring-opened intermediate can react along two parallel pathways, by either dissociation of glycinate or protonation of the NH_2 group followed by dissociation of the zwitterion. The rapid fluoride and glycinate exchange results in the loss of spin−spin coupling between the coordinated fluorides.

The dissociation of fluoride takes place along a separate pathway with the rate constant k_4. The rate law for the glycine exchange deduced from this mechanism is[33−35]

$$k_{obs} = \frac{k_1 k_3 K[H^+]}{k_{-1} + k_3 K[H^+]} \qquad (13)$$

We have neglected the pathway described by k_2, which is slower than the proton-assisted reaction, as indicated by comparison with the experimental rate law. The reciprocal plot of eq 12 (see Figure 5) is linear with an intercept $1/k_1$ and a slope k_{-1}/k_1k_3K. From these quantities, we obtain for k_1 129 ± 3 and 143 ± 2 s^{-1} and for k_{-1}/k_3K (2.3 ± 0.1) × 10^{-9} and (0.14 ± 0.02) × 10^{-9} M s in H_2O and D_2O, respectively.

(32) Reeves, L. W.; Shaw, K. N. *Can. J. Chem.* **1970**, *48*, 3641.
(33) Basolo, F.; Hayes, J. C.; Neumann, H. M. *J. Am. Chem. Soc.* **1954**, *76*, 3807.
(34) Curtis, N. F.; Osvath, S. R. *Inorg. Chem.* **1988**, *27*, 305.
(35) Yeh, A.; Taube, H. *J. Am. Chem. Soc.* **1980**, *102*, 4725.

Scheme 2

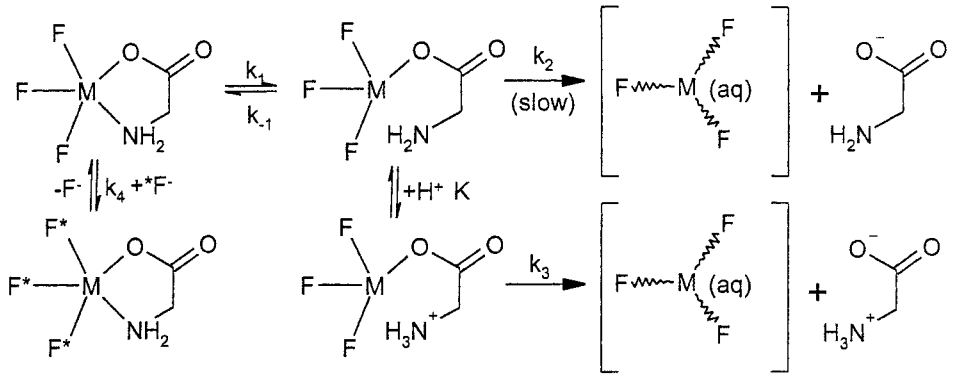

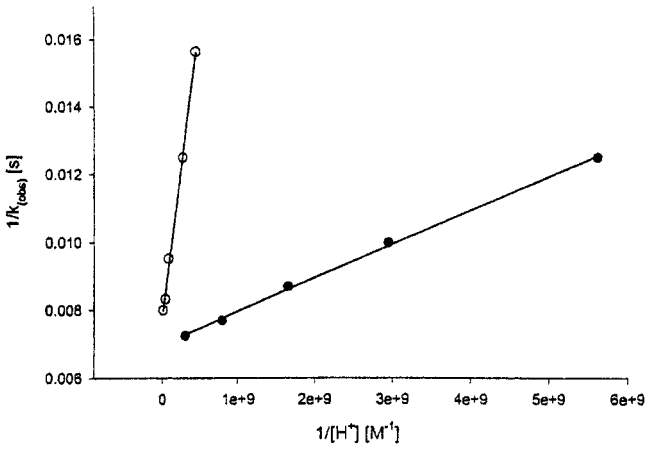

Figure 5. Plot of $1/k_{obs}$ (● in D_2O, ○ in H_2O) against $1/[H^+]$ for glycine exchange in $UO_2(glycine)F_3^{2-}$.

The rate constant for the ring opening, k_1, is independent of the solvent and is of the same magnitude as that found in the picolinate system. There is a large reverse isotope effect on the subsequent steps in the mechanism, indicating H^+/D^+ bonding to the "free" NH_2 group. This interpretation is supported by the activation parameters for the glycine exchange, $\Delta H^{\ddagger} = 90 \pm 10$ kJ/mol and $\Delta S^{\ddagger} = 120 \pm 30$ J/K mol. These values are approximate and were calculated from the temperature dependence of the fluoride signals in the complex, assuming that the change in line shape is mainly due to the glycinate exchange. The activation entropy is similar to the one found for the proton-catalyzed exchange in the binary U(VI)−carbonate system.[36]

The next issue is to decide whether the "UO_2F_3" intermediate in Scheme 2 is identical with the known complex $UO_2F_3(H_2O)_2^-$. This was done by investigating whether the line width of the ^{19}F NMR signal of $UO_2F_3(H_2O)_2^-$ was independent of the equilibrium concentration of free glycine. The fact that the line width remained constant indicates that the back reaction between "UO_2F_3" and glycine is independent of the concentration of $UO_2F_3(H_2O)_2^-$; that is, the two species are not identical. "UO_2F_3" is an intermediate whose coordination geometry differs from that of the species in the α-hydroxyisobutyrate system discussed above.

In the following section, we will make a comparison between the rates of exchange of glycine discussed above and those of glycolate in complexes of type **9**. Because of the low concentration of the glycolate complex, we could not measure the rates of exchange; the only experimental information available is a slight broadening of the fluoride peaks with decreasing pH and the absence of spin−spin coupling. The latter indicates that either the rate of fluoride exchange or the rate of ring opening/dissociation of oxoacetate is higher than 30−35 s^{-1}, estimated from the typical spin−spin coupling in ternary carboxylate−fluoride complexes.[2] Because the rates of ligand exchange do not vary much among different ternary complexes,[1−3] we will use the experimental information from the glycolate complex **11**, found at higher pH, for the comparison with the glycinate complex **9**. The ^{19}F line width of complex **11** is constant in the pH range 7−8.5, where the rate of fluoride exchange was measured as 12 s^{-1}. The rate of glycolate exchange was 1.2 s^{-1} at pH = 8.5. Both these rates are lower than that required for the loss of spin−spin coupling in the glycolate complex **9**. Previous experimental data[2] show that the rate of dissociation of the fluoride does not change significantly in the pH range 7−8.5. The most likely explanation for the observed loss of spin−spin coupling in the glycolate complex **9** in the pH range 6.8−7.2 is a proton-catalyzed glycolate exchange. Previous studies[2] of the carbonate analogue of complex **9** indicate that a change from pH 8.5 to 7 will increase the rate of exchange of carbonate by more than 1 order of magnitude. We infer from this that a similar increase in the rate of exchange may also occur for the glycolate exchange in **9**. The experimental data for **9** and **11** are consistent with both the mechanism proposed for the glycine system and a mechanism involving a proton-catalyzed ring-opening reaction. For the latter mechanism, the rate constant is equal to

$$k_{obs} = \frac{k_0 + K_o k_1 [H^+]}{1 + K_o [H^+]} \qquad (14)$$

which has the same form as eq 13 if k_0, the rate constant for the (proton-independent) ring opening, is small. K_o is the equilibrium constant for the (fast) protonation of the coordinated oxoacetate ligand, and k_1 is the rate constant for the dissociation of the protonated ligand. For complex **11**, we can obtain experimental data only at high pH, where k_0 is the predominant term. For complex **9**, we have data at lower pH indicating that the H^+-dependent terms also contribute. From the available information, we conclude that k_0 is less than 1.2 s^{-1}. The oxoacetate has electron pairs available for proton attack. In addition, it is a much stronger base than the corresponding glycine complex. Both these facts make a proton-catalyzed ring opening more plausible than a ring opening followed by protonation as in the glycine system.

(36) Bányai, I.; Glaser, J.; Micskei, K.; Tóth, I.; Zékány, L. *Inorg. Chem.* **1995**, *34*, 3785.
(37) Ahrland, S.; Kullberg, L. *Acta Chem. Scand.* **1971**, *25*, 3457.

Conclusions and Comparison with Earlier Work

We can now present a coherent picture of the mechanisms for ligand substitution in the uranium(VI) complexes investigated:

The ligand exchange in all ternary complexes investigated seems to follow two parallel pathways, one for fluoride and the other for the bidentate ligand L. In each complex, the rate constant and the activation parameters for the dissociation of fluoride are not strongly dependent on L.

The substitution of chelate-bonded L involves two consecutive reactions, a chelate ring opening which is followed by dissociation. There is no proton catalysis in the ring-opening step for ligands such as picolinate and glycinate, which do not have free electron pairs when coordinated. The first step also involves a ring opening in ligands containing free electron pairs, such as carbonate, oxalate, and oxoacetate. However, this is proton-catalyzed with indications of a parallel non-proton-assisted pathway.

The rate constant for the ring opening is correlated with the donor strength of the coordinated ligand, with the smallest values for coordinated oxoacetate and oxalate, with a charge of −2. In the same way, the rate constant decreases with increasing donor strength of the nitrogen, but the difference is smaller than expected between aliphatic and aromatic amines.

In the acetate, glycolate, and α-hydroxyisobutyrate complexes **8**, in which the ligand is bonded only at the carboxylate end, the exchange reaction seems to follow an Eigen−Wilkins mechanism. The situation is different for the other ligands (carbonate and glycine), for which the intermediate "UO_2F_3" is not identical with $UO_2F_3(H_2O)_2^-$.

Acknowledgment. This project has been financially supported by contributions from KTH and the authors. A contribution for travel expenses from the Frans Georg and Gull Liljenroth Foundation is gratefully acknowledged. This paper is dedicated to the memory of Sten Ahrland, who was the supervisor, life-long friend, and mentor to I.G..

Supporting Information Available: Titration curves for the binary and ternary systems investigated at various U(VI) and ligand concentrations (S1 and S2), pH-dependent ^{17}O and ^{1}H NMR spectra and equilibrium U(VI) distribution diagram as a function of pH for the U(VI)−glycolate system (S3 and S4), pH dependence of the ^{17}O and ^{1}H NMR spectra for the U(VI)−glycolate−fluoride system (S5 and S6), plots of the observed rate constants against the equilibrium glycolate and α-hydroxyisobutyrate concentrations for **6** in the binary glycolate system and $UO_2F_3^-$ in the ternary α-hydroxyisobutyrate−fluoride system (S7), Eyring plot of the temperature dependence of the rate constant for the exchanges between $UO_2(glyc)_2F^{3-}$ and free fluoride or free glycolate (S8), pH-dependent ^{17}O NMR spectra and equilibrium distribution diagram for the U(VI)−α-hydroxyisobutyrate system (S9), pH-dependent ^{19}F NMR spectra and equilibrium distribution diagram for the U(VI)−α-hydroxyisobutyrate−fluoride system (S10 and S11), pH dependence of the ^{19}F NMR spectra and equilibrium distribution diagram for the U(VI)−glycine−fluoride system (S12), proton concentration dependence of the pseudo-first-order rate for glycine exchange in the $UO_2(H_2N-CH_2-COO)F_3^{2-}$ complex (S13), and temperature-dependent ^{19}F NMR spectra in the U(VI)−glycine−fluoride system and Eyring plot of the temperature dependence of the rate constant for the glycine exchange (S14). This material is available free of charge via the Internet at http://pubs.acs.org.

IC000400N